



# CHORUS

This is the accepted manuscript made available via CHORUS. The article has been published as:

## Probing Configuration Mixing in $^{12}\text{Be}$ with Gamow-Teller Transition Strengths

R. Meharchand, R. G. T. Zegers, B. A. Brown, Sam M. Austin, T. Baugher, D. Bazin, J. Deaven, A. Gade, G. F. Grinyer, C. J. Guess, M. E. Howard, H. Iwasaki, S. McDaniel, K. Meierbachtol, G. Perdikakis, J. Pereira, A. M. Prinke, A. Ratkiewicz, A. Signoracci, S. Stroberg, L. Valdez, P. Voss, K. A. Walsh, D. Weisshaar, and R. Winkler

Phys. Rev. Lett. **108**, 122501 — Published 19 March 2012

DOI: [10.1103/PhysRevLett.108.122501](https://doi.org/10.1103/PhysRevLett.108.122501)

# Probing configuration mixing in $^{12}\text{Be}$ with Gamow-Teller transition strengths

R. Meharchand,<sup>1,2,3,\*</sup> R.G.T. Zegers,<sup>1,2,3,†</sup> B.A. Brown,<sup>1,2</sup> Sam M. Austin,<sup>1,3</sup> T. Baugher,<sup>1,2</sup> D. Bazin,<sup>1</sup> J. Deaven,<sup>1,2,3,‡</sup> A. Gade,<sup>1,2</sup> G.F. Grinyer,<sup>1,§</sup> C.J. Guess,<sup>1,2,3,¶</sup> M.E. Howard,<sup>3,4,5</sup> H. Iwasaki,<sup>1,2</sup> S. McDaniel,<sup>1,2</sup> K. Meierbachtol,<sup>1,6</sup> G. Perdikakis,<sup>1,3</sup> J. Pereira,<sup>1,3</sup> A.M. Prinke,<sup>1,2,3</sup> A. Ratkiewicz,<sup>1,2</sup> A. Signoracci,<sup>1,2,\*\*</sup> S. Stroberg,<sup>1,2</sup> L. Valdez,<sup>1,2,3</sup> P. Voss,<sup>1,2,††</sup> K.A. Walsh,<sup>2</sup> D. Weisshaar,<sup>1</sup> and R. Winkler<sup>1,‡‡</sup>

<sup>1</sup>*National Superconducting Cyclotron Laboratory, Michigan State University, East Lansing, Michigan 48824-1321, USA*

<sup>2</sup>*Department of Physics and Astronomy, Michigan State University, East Lansing, Michigan 48824, USA*

<sup>3</sup>*Joint Institute for Nuclear Astrophysics, Michigan State University, East Lansing, Michigan 48824, USA*

<sup>4</sup>*Department of Physics and Astronomy, Rutgers University, Piscataway, New Jersey 08854, USA*

<sup>5</sup>*Oak Ridge National Laboratory, Oak Ridge, Tennessee 37831, USA*

<sup>6</sup>*Department of Chemistry, Michigan State University, East Lansing, Michigan 48824, USA*

We present a novel technique for studying the quenching of shell gaps in exotic isotopes. The method is based on extracting Gamow-Teller ( $\Delta L=0$ ,  $\Delta S=1$ ) transition strengths [ $B(\text{GT})$ ] to low-lying states from charge-exchange reactions at intermediate beam energies. These Gamow-Teller strengths are very sensitive to configuration mixing between cross-shell orbitals, and this technique thus provides an important complement to other tools currently used to study cross-shell mixing. This work focuses on the  $N = 8$  shell gap. We populated the ground and 2.24 MeV  $0^+$  states in  $^{12}\text{Be}$  using the  $^{12}\text{B}(1^+)(^7\text{Li},^7\text{Be})$  reaction at 80 MeV/ $u$  in inverse kinematics. Using the ground-state  $B(\text{GT})$  value from  $\beta$ -decay measurements ( $0.184 \pm 0.007$ ) as a calibration, the  $B(\text{GT})$  for the transition to the second  $0^+$  state was determined to be  $0.214 \pm 0.051$ . Comparing the extracted Gamow-Teller strengths with shell-model calculations, it was determined that the wave functions of the first and second  $0^+$  states in  $^{12}\text{Be}$  are composed of  $25 \pm 5\%$  and  $60 \pm 5\%$   $(0s)^4(0p)^8$  configurations, respectively.

PACS numbers: 21.60.Cs, 23.20.Lv, 25.60.Lg, 25.70.Kk,

Light unstable isotopes provide fertile testing grounds for studying the evolution of nuclear structure away from the valley of stability, as exotic phenomena such as halos, Borromean systems, parity inversions of low-lying states, and the disappearance of conventional magic numbers can be found in isotopes with only a few neutrons more than stable species. The disappearance of the magic numbers is associated with a quenching of a shell gap between single-particle orbitals that are well-separated in stable isotopes. In this Letter, we introduce a new method for quantifying the degree of quenching by measuring the configuration mixing between orbitals on either side of the gap. This is done by extracting the Gamow-Teller (GT) transition strengths [ $B(\text{GT})$ ] to low-lying states of the exotic nucleus using a charge-exchange (CE) reaction at intermediate energy. The method provides a valuable addition to the other techniques used to study shell quenching, since the magnitudes of the extracted GT strengths are strongly correlated with the extent of the configuration mixing, but the analysis procedures used to extract GT strengths from the data are insensitive to a-priori assumptions on the mixing. Here, we employ the ( $^7\text{Li},^7\text{Be}$ ) CE reaction at 80 MeV/ $u$  on  $^{12}\text{B}$  to study the quenching of the  $N = 8$  gap in  $^{12}\text{Be}$ .

The case of  $^{12}\text{Be}$  has already been the subject of extensive experimental and theoretical work. Low-lying states with spin-parity  $2_1^+$  ( $E_x=2.11$  MeV),  $0_2^+$  ( $E_x=2.24$  MeV,  $\tau=331$  ns), and  $1_1^-$  ( $E_x=2.68$  MeV) provide strong signatures of shell quenching [1–7], yet the level of mixing between  $p$  and  $sd$  shell configurations remains the subject

of intense debate. This is despite the large body of data available from  $(t,p)$  [1, 3], neutron knockout [8, 9], inelastic scattering [4, 5], and  $(d,p)$  [10] experiments. The current study addresses a particularly controversial aspect of the discussion [11–15], the relative contributions of  $(0s)^4(0p)^8$  “ $0\hbar\omega$ ” and  $(0s)^4(0p)^6(1s0d)^2$  “ $2\hbar\omega$ ” configurations to the  $0^+$  states of  $^{12}\text{Be}$ .

Most calculations performed prior to 2010 agree that the ground state of  $^{12}\text{Be}$  is dominated by  $2\hbar\omega$  configurations. The shell-model calculations of Barker [11, 13] predict that  $2\hbar\omega$  components make up 69% of the ground state wavefunction. These results are consistent with the predictions produced by a model developed by Fortune and Sherr based on Coulomb shifts (68%  $2\hbar\omega$ ) [12, 14, 15]. ( $^{10}\text{Be}+n+n$ ) three-body calculations performed by Romero-Redondo *et al.* [16] predict an even stronger  $2\hbar\omega$  component (71–87%). Overall, these predictions are in good agreement with results from neutron knockout measurements performed in 2000 and 2006 [8, 9], in which 68% of the ground state wavefunction was estimated to consist of  $2\hbar\omega$  configurations. Recently, however, particle-particle random-phase approximation (pp-RPA) [17] and microscopic No-Core Shell-Model (NCSM) calculations [18] have predicted ground state wavefunctions dominated by  $0\hbar\omega$  configurations (75% and 59%, respectively), in conflict with the earlier predictions and the knockout measurements. In addition, the pp-RPA calculations and Barker’s shell-model calculations [11, 13] predict that the 2.24  $0_2^+$  state in  $^{12}\text{Be}$  is primarily made up of  $2\hbar\omega$  configurations. This is in

agreement with a 2010  $^{11}\text{Be}(d,p)$  measurement [10], but conflicts with the aforementioned calculations of Fortune and Sherr [14, 15] and Romero-Redondo *et al.*[16], which predict  $0\hbar\omega$  dominance for the 2.24 MeV  $0^+$  state. In Ref. [15] the validity of the results of the recent  $^{11}\text{Be}(d,p)$  experiment [10], in which a  $s$ -wave spectroscopic factor of  $0.28_{-0.07}^{+0.03}$  ( $0.73_{-0.40}^{+0.27}$ ) for the  $0_1^+$  ( $0_2^+$ ) was extracted, are questioned. Clearly, more information is needed to precisely quantify configuration mixing in the  $0^+$  states of  $^{12}\text{Be}$  and to resolve the inconsistencies between the existing data and various theoretical models.

Much of the information obtained to date regarding configuration mixing in  $^{12}\text{Be}$  is based on methods that are sensitive to the  $2\hbar\omega$  component of the wavefunction. As first suggested in Ref. [19], a measurement of GT strengths from the ground state of  $^{12}\text{B}$  to states in  $^{12}\text{Be}$  would provide complementary information on the  $0\hbar\omega$  component of each state. This provides valuable insight, a check on the previous measurements, and an additional observable with which to test theoretical models.

Here, we report on the first measurement of the Gamow-Teller strength for the 2.24 MeV  $0_2^+$  state in  $^{12}\text{Be}$  using the  $^{12}\text{B}(^7\text{Li}, ^7\text{Be})^{12}\text{Be}$  CE reaction in inverse kinematics. Since the  $^{12}\text{B}(1^+)$  ground state is predominantly made up of  $0\hbar\omega$  configurations (83%, based on calculations discussed below), the Gamow-Teller ( $\Delta L=0$ ,  $\Delta S=1$ ) strength to the  $0^+$  states in  $^{12}\text{Be}$  is a reflection of the  $0\hbar\omega$  component in their wavefunctions. Using a well-known proportionality between the CE cross section (at zero momentum transfer  $q$ ) and  $B(\text{GT})$  [20],

$$\left. \frac{d\sigma}{d\Omega} \right|_{q=0} = \hat{\sigma} B(\text{GT}), \quad (1)$$

one can calibrate the unit cross section  $\hat{\sigma}$ , as the  $^{12}\text{Be}(\text{g.s.}) \rightarrow ^{12}\text{B}(\text{g.s.})$   $B(\text{GT})$  is known from  $\beta$ -decay [21]. The unit cross section can then be applied to extract the  $B(\text{GT})$  for the  $0_2^+$  state. By comparing the measured strengths to shell model predictions one can determine the  $0\hbar\omega$  component of the  $0^+$  states' wavefunctions.

The experiment was performed at the NSCL Coupled Cyclotron Facility. A 120 MeV/ $u$  beam of  $^{18}\text{O}^{8+}$  was impinged upon a 1904 mg/cm<sup>2</sup> thick  $^9\text{Be}$  target. An 80 MeV/ $u$   $^{12}\text{B}$  secondary beam (with purity exceeding 99%) was separated from other fragmentation products using a 405 mg/cm<sup>2</sup> thick aluminum wedge placed at the intermediate image of the A1900 fragment separator [22]. The momentum acceptance of the separator was  $\pm 0.25\%$ , resulting in a secondary  $^{12}\text{B}$  beam intensity of  $3 \times 10^6 \text{ s}^{-1}$ .

The experimental setup was similar to that described in Ref. [23]. A 5.5 mg/cm<sup>2</sup>  $^{nat}\text{Li}$  target was placed at the pivot point of the S800 spectrograph [24]. Dispersion-matched optics were employed in order to achieve optimal energy resolution for  $^{12}\text{Be}$  nuclei detected in the spectrograph. Reaction products were identified and measured on an event-by-event basis using a suite of detectors in the S800 focal plane [25]. Angles and positions in the

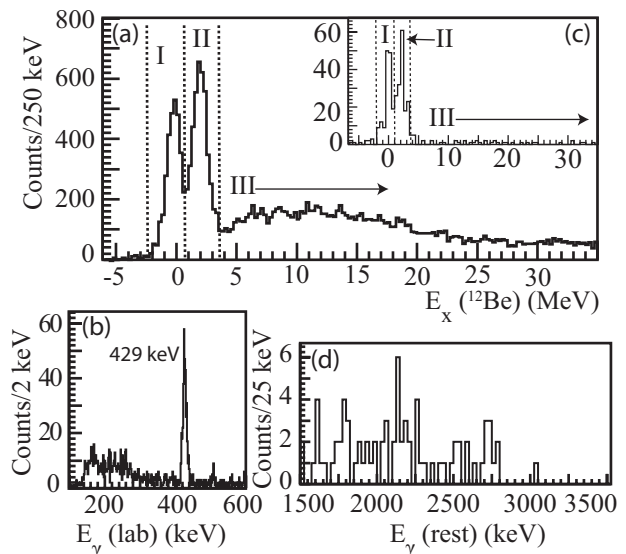


FIG. 1. (a) Excitation-energy spectrum of  $^{12}\text{Be}$ , excited via the  $^{12}\text{B}(^7\text{Li}, ^7\text{Be})$  reaction at 80 MeV/ $u$  and gated on  $^{12}\text{Be}$  particles detected in the spectrograph. (b) Laboratory  $\gamma$ -energy spectrum gated on  $^{12}\text{Be}$  particles detected in the spectrograph. (c) Same as (a), but also gated on 429 keV  $\gamma$  rays in (b). (d) Doppler-reconstructed  $\gamma$ -ray energy spectrum, gated on region II in (a).

dispersive and non-dispersive planes were measured using two Cathode Readout Drift Counters (CRDCs). Particle identification was performed by combining the relative time-of-flight (between a 3-mm thick plastic scintillator located in the S800 focal plane and the CCF radio-frequency signal), and the energy-loss signal from a 5-mm thick plastic scintillator also placed in the focal plane. A 5<sup>th</sup>-order raytrace matrix was used to reconstruct the center-of-mass scattering angle and, after a missing-mass calculation, the excitation energy of  $^{12}\text{Be}$ . The  $^{12}\text{B}^{4+}$  charge state, produced when  $^{12}\text{B}^{5+}$  ions pick up an electron in the target, was used to estimate the intrinsic kinetic energy resolution of 900 keV (FWHM) and the angular resolutions in the dispersive and non-dispersive planes of 12 and 9 mrad, respectively.

Photons emitted from excited states populated in the reaction were detected in the Segmented Germanium Array (SeGA) [26]. Fifteen, 32-fold segmented high-purity Ge detectors were arranged in a closely-packed configuration around the target, with crystal axes parallel to the beam axis and at a distance of 13.2 cm, covering laboratory polar angles between  $40^\circ$  and  $140^\circ$ . The  $\gamma$ -ray photopeak detection efficiency, determined with standard sources, ranged from 17% at  $E_\gamma = 250$  keV to 3.5% at  $E_\gamma = 2.5$  MeV. The segmentation of SeGA is aimed at minimizing the uncertainty in the  $\gamma$  emission angle, improving the energy resolution of the Doppler-reconstructed  $\gamma$ -energy spectrum (the decaying nuclei travel at  $\beta = 0.39c$ ). However, because

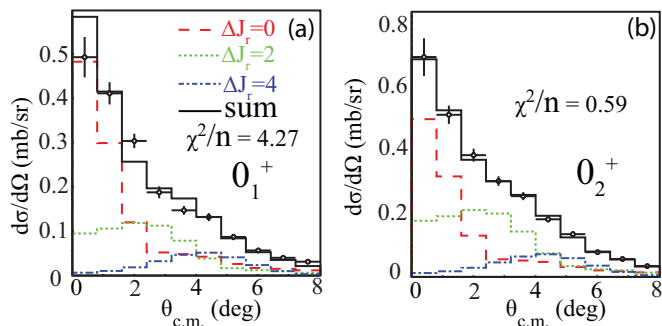


FIG. 2. (color online) Differential cross sections for the  $^{12}\text{B}(^7\text{Li}, ^7\text{Be})$  reaction populating (a) the  $0_1^+$  and (b)  $0_2^+$  states of  $^{12}\text{Be}$ . The results of the MDA are also shown in the figures, together with the quality of the fit, expressed in terms of the  $\chi^2$  per degree of freedom ( $n$ ). The  $\Delta J_r = 0$  component corresponds to the GT contribution to the excitation.

dispersion-matched optics were used in this experiment, the beamspot at the target was 5 cm wide in the dispersive plane. Since the hit position on the target in this plane cannot be reconstructed in the raytrace procedure, the large beamspot resulted in a large uncertainty in the  $\gamma$ -ray emission angle, and the energy resolution for Doppler-reconstructed  $\gamma$  rays was limited to 7%.

The  $^{12}\text{Be}$  singles (spectrograph only) excitation-energy spectrum is shown in Fig. 1(a). Clearly visible are the  $^{12}\text{Be}$  ground state peak (region I), another peak centered at  $\sim 2$  MeV (region II), and a broad feature at higher excitation energy (region III). Since this spectrum is not gated on  $\gamma$  rays, it contains events associated with various transitions in the  $^7\text{Li}$ - $^7\text{Be}$  and  $^{12}\text{B}$ - $^{12}\text{Be}$  systems. Considering first the  $^7\text{Li}$ - $^7\text{Be}$  system: only the  $^7\text{Li} \rightarrow ^7\text{Be}_0(\frac{3}{2}^-)$ , ground state) and  $^7\text{Li} \rightarrow ^7\text{Be}_1(\frac{1}{2}^-)$ , 429 keV) transitions can contribute to the  $^{12}\text{Be}$  excitation-energy spectrum below 3.5 MeV (regions I and II) since the second excited state in  $^7\text{Be}$  lies at 4.57 MeV. Considering the  $^{12}\text{B}$ - $^{12}\text{Be}$  system, any  $^{12}\text{Be}$  excitations beyond the neutron separation threshold of 3.69 MeV would not be associated with  $^{12}\text{Be}$  events in the spectrograph. Therefore, events observed in region III of Fig. 1(a) must originate from reactions producing  $^{12}\text{Be}$  but in which neither the  $^7\text{Be}_0$  (ground state) nor  $^7\text{Be}_1$  (429 keV) levels were populated. To confirm this, we gated the  $^{12}\text{Be}$  excitation-energy spectrum on the 429 keV  $\gamma$ -ray emitted in the  $^7\text{Be}_1 \rightarrow ^7\text{Be}_0$  de-excitation [shown in Fig. 1(b)]. This  $\gamma$ -gated excitation-energy spectrum is shown in Fig. 1(c), and virtually no events were observed in region III, despite the similarities observed for regions I and II. Thereby convinced that region III events are not relevant to the  $0^+$  states in  $^{12}\text{Be}$  under investigation here, we excluded them from further consideration.

$^{12}\text{Be}$  has three states that can contribute to the  $\sim 2$  MeV peak seen in region II of Fig. 1(a):  $2_1^+$  (2.11 MeV),  $0_2^+$  (2.24 MeV), and  $1_1^-$  (2.68 MeV). The  $2_1^+$  and  $1_1^-$  lev-

els de-excite to the ground state by  $\gamma$ -ray emission. The  $\gamma$ -ray yields associated with these transitions were only weakly visible in the Doppler-corrected  $\gamma$ -energy spectrum gated on region II, as shown in Figure 1(d). By counting the number of events possibly associated with the photopeaks due to the decay of the  $2_1^+$  and the  $1_1^-$  levels in this spectrum (events within  $\pm 2\sigma_{\text{resolution}}$  were used) upper limits to region II were determined. Since the spectrum of Fig. 1(d) is not free of background, a correction to these limits was made by subtracting the number of events in the same photopeak windows but gated on region I of Fig. 1(a). After correcting for the photopeak efficiencies, upper limits for the contributions to region II of Fig. 1(a) of  $7 \pm 2\%$  and  $4 \pm 1\%$  due to the excitation of the  $2_1^+$  and the  $1_1^-$  states were established.

The widths of the peaks in regions I and II of Fig. 1(a) are both  $1.6 \pm 0.1$  MeV (FWHM). This is broader than the intrinsic kinetic energy resolution due to difference in energy loss of the projectile and ejectile in the target, the uncertainty in the scattering angle which contributes to the uncertainty of the missing mass calculation and because  $^7\text{Be}_0$  and  $^7\text{Be}_1$  final states both contribute. The short lifetimes of the  $2_1^+$  and  $1_1^-$  levels ensure a prompt  $\gamma$  decay near the target and the associated momentum kick broadens the width of the  $\sim 2$  MeV peak in Fig. 1(a). If this peak were solely due to the  $2^+$  or  $1^-$  state, its width would be  $\sim 2.3$  MeV. Such a broadening will not occur for the excitation of the isomeric  $0_2^+$  level since it has a lifetime of  $331 \pm 12$  ns [6] and the associated  $^{12}\text{Be}$  ions are unlikely to decay before reaching the S800 focal plane. Because the contribution of the  $2_1^+$  and the  $1_1^-$  states to region II are small, and the peak widths are sensitive to several other parameters that carry uncertainties, quantifying the level of contamination from these levels was not meaningful compared to the extraction from the  $\gamma$ -spectrum. Nevertheless, the fact that the widths of peaks I and II are equal provides further support for  $0_2^+$  dominance of the  $\sim 2$  MeV peak.

Confident that the ground state ( $0_1^+$ ) and 2.24 MeV ( $0_2^+$ ) states in  $^{12}\text{Be}$  dominate the peaks of region I and II, the high-statistics singles data of Fig 1(a) was used to extract GT strengths. A similar analysis with the  $\gamma$ -coincident data of Fig. 2(c) was also performed, yielding consistent results, but with large statistical uncertainties.

The differential cross sections extracted from the singles data for the excitation of the  $0_1^+$  and  $0_2^+$  states in  $^{12}\text{Be}$  are plotted in Fig. 2(a) and (b), respectively. Eq. (1) for the extraction of  $B(\text{GT})$  is only valid if applied to the  $\Delta L=0$ ,  $\Delta S=1$ ,  $\Delta J=1$  (GT) component of the cross section. Due to the internal structure of both the projectile and the target, and the fact that the cross section is integrated over the  $^7\text{Li} \rightarrow ^7\text{Be}_0$  and  $^7\text{Li} \rightarrow ^7\text{Be}_1$  excitations, contributions with relative total angular momentum transfer ( $\Delta J_r = \Delta J_t + \Delta J_p$ ) up to 4 can contribute, where  $\Delta J_t$  ( $\Delta J_p$ ) is the total angular momentum transfer in the target (projectile). Only the  $\Delta J_r = 0$  ( $\Delta J_t = 1$

and  $\Delta J_p = 1$ ) is relevant for extracting GT strengths.

To extract the  $\Delta J_r = 0$  component from the data, a multipole decomposition analysis (MDA) was performed, using differential cross sections calculated in the Distorted Wave Born Approximation (DWBA) with the FOLD code [27]. Transition densities were calculated using the shell-model code OXBASH [28]. The CKII interaction [29] was used in the  $p$ -shell model space to calculate the transition densities for the  ${}^7\text{Li}$ - ${}^7\text{Be}$  system, and the WBP interaction [30] was used in the  $sp\text{sd}p\text{f}$ -shell model space to calculate the transition densities for the  ${}^{12}\text{B}$ - ${}^{12}\text{Be}$  system. It is important to note that the angular distributions associated with different units of total angular momentum transfer do not depend significantly on the choice of the shell-model interaction or model-space, but predominantly on the value of  $\Delta J_r$ .

The effective nucleon-nucleon interaction of Ref. [31] was double-folded over the transition densities to produce separate form factors for each multipole. In the DWBA calculation, optical potentials from Ref. [32] were used. The DWBA cross sections were smeared with the experimental angular resolution and re-binned to match the binning of the experimental angular distributions. The experimental angular distributions were then fit with a linear combination of DWBA multipole components to determine the  $\Delta J_r=0$  cross section at zero degrees, as shown in Fig. 2. Contributions from  $\Delta J_r = 1$  and  $\Delta J_r = 3$  components (they peak just below  $2^\circ$  and at  $3.5^\circ$ , respectively and have a relatively deep minimum at  $0^\circ$ ), which are associated with the excitation of the  $1^-$  state, were found to be consistent with zero and are not shown in Fig. 2(b). However, within uncertainties, a contribution of the  $1^-$  state at the level of the upper limit deduced from the  $\gamma$ -ray spectrum of Fig. 1(d) was not excluded. To ensure that a small contamination of the  $0_2^+$  state from the  $2_1^+$  state did not strongly bias the results (both excitations have a  $\Delta J_r = 0$  contribution), the ratio of events in region II to events additionally gated on the 2.11 MeV photopeak in spectrum Fig. 1(d) was determined, separately for  $\theta_{c.m.} < 2.4^\circ$  and  $\theta_{c.m.} > 2.4^\circ$ . Since these ratios in the two angular regions were consistent with each other, a strong bias was excluded.

The zero-degree  $\Delta J_r = 0$  cross sections extracted from the MDA were extrapolated to  $q = 0$  based on the DWBA calculations, following the procedure described e.g. in Ref. [33]. The unit cross section in Eq. (1) was calibrated using the  ${}^{12}\text{B}(\text{g.s.}) \rightarrow {}^{12}\text{Be}(0_1^+)$  transition, since the corresponding  $B(\text{GT})$  is known from  $\beta$ -decay data ( $B(\text{GT})=0.184 \pm 0.008$  [21]). We found that  $\hat{\sigma} = 3.72 \pm 0.34$  mb/sr. Applying this unit cross section to the  $\Delta J_r = 0$  cross section at  $q = 0$  for the excitation of the  $0_2^+$  state results in a  $B(\text{GT})$  of  $0.214 \pm 0.051$ . The error cited for the  $0_2^+$  state includes: statistical and MDA fitting errors (8% error for the  $0_1^+$  state, 9% for the  $0_2^+$  state, after propagation through the  $q=0$  extrapolation and conversion to  $B(\text{GT})$ ); and systematic errors

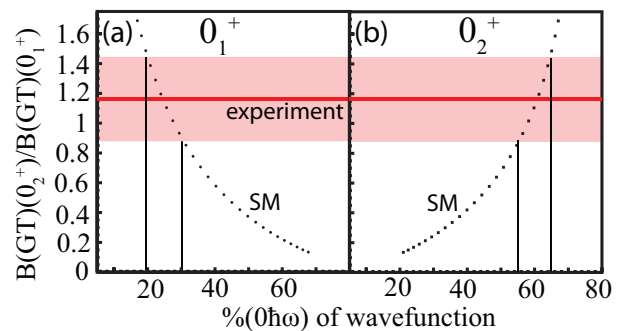


FIG. 3. (color online) Ratio of  $0_2^+$  to  $0_1^+$   $B(\text{GT})$  values, plotted as a function of the percentage of the (a)  $0_1^+$  and (b)  $0_2^+$  state wavefunction that consist of  $0\hbar\omega$  configurations. The red line indicates the  $B(\text{GT})$  ratio found in the current work; the shaded area is the error associated with this experimental ratio. The vertical bands correspond to the extracted percentages of  $0\hbar\omega$  content (see text).

from the peak-fitting procedure used to generate experimental angular distributions (4%), the smearing procedure of DWBA differential cross sections (1%), the uncertainty in the extrapolation to  $q=0$  (1%), and the effects of the tensor interaction in the charge-exchange reaction mechanism (11%). The last contribution was estimated by comparing the calculated cross sections with ones in which the tensor component of the Love-Franey interaction was switched off, following the procedure discussed in e.g. Ref. [34]. Since the upper limit for the contamination of the  $0_2^+$  state from the excitation of the  $2_1^+$  state is small compared to the combination of the other uncertainties, it did not significantly affect the results.

Information regarding the microscopic structure of the  $0_1^+$  and  $0_2^+$  states in  ${}^{12}\text{Be}$  can be extracted by comparing the ratio of the experimental GT strengths,  $R_{B(\text{GT})} = \frac{B(\text{GT})(0_2^+, 2.24 \text{ MeV})}{B(\text{GT})(0_1^+, \text{g.s.})}$ , to the theoretical ratio and incorporating different assumptions for the mixing between  $0\hbar\omega$  and  $2\hbar\omega$  configurations. This is shown in Fig. 3 - each point represents a shell-model calculation using the WBP interaction [30] in the  $sp\text{sd}p\text{f}$  model space, where the energies of all  $2\hbar\omega$  configurations have been augmented by an amount  $\Delta E$  to adjust the amount of configuration mixing between  $0\hbar\omega$  and  $2\hbar\omega$  configurations. The  $\Delta E$  values used for calculating the points shown in Figure 3 varied from -2.0 MeV to -5.0 MeV, in steps of -0.1 MeV. The calculations are presented as the percentage of the wavefunction made up of  $0\hbar\omega$  configurations - as  $\Delta E$  becomes more negative, the  $0\hbar\omega$  fraction of the  $0_1^+$  state wavefunction becomes smaller [Fig. 3(a)], and that of  $0_2^+$  state [Fig. 3(b)] wavefunction becomes larger.

The value of  $R_{B(\text{GT})}$  extracted from the data was  $1.162 \pm 0.283$ , as indicated by shaded bars in Figs. 3(a,b). Note that since  $\hat{\sigma}$  is divided out in the calculation of  $R_{B(\text{GT})}$ , errors associated with the absolute value of  $\hat{\sigma}$  do

not contribute to the error of  $R_{B(GT)}$ . The shell-model calculations reproducing this ratio yield wavefunctions in which the  $0_1^+(0_2^+)$  state is comprised of  $25\pm 5\%$  ( $60\pm 5\%$ )  $0\hbar\omega$  configurations. The  $0\hbar\omega$  contributions do not sum to 100% since there is also a small amount of mixing with higher  $0^+$  states. In terms of orbital occupancies it is customary to use the  $2\hbar\omega$  component of  $75\pm 5\%$  ( $40\pm 5\%$ ) to provide the neutron  $sd$ -shell occupancy of  $\langle \nu_{sd} \rangle = 1.50\pm 30$  ( $0.80\pm 16$ ) for the  $0_1^+(0_2^+)$  states.

Recently a new Hamiltonian for the full  $p - sd$  model space has been developed by Utsuno and Chiba [35]. The  $B(GT)$  values obtained with this Hamiltonian give  $R_{B(GT)} = 2.91$  and a neutron  $sd$  shell occupancy of  $\langle \nu_{sd} \rangle = 1.88$  ( $0.67$ ) for the  $0_1^+(0_2^+)$  states. Agreement with experiment can be obtained by increasing the  $p - sd$  shell gap by 1 MeV in the Utsuno-Chiba Hamiltonian to give  $R_{B(GT)} = 1.18$  and  $\langle \nu_{sd} \rangle = 1.52$  ( $0.82$ ).

We conclude that the spectroscopic properties obtained by combining these experimental results with shell-model calculations, independent of whether the older  $(0+2)\hbar\omega$  basis with the WBP interaction or the full  $p - sd$  basis with the Utsuno-Chiba Hamiltonian is used, agree within  $2\sigma$  with previous neutron knockout measurements [8, 9], but the  $0_2^+$  wavefunction conflicts with the conclusions of the recent  $(d,p)$  transfer measurement of Ref. [10], confirming the reservations of that result expressed in Ref. [15].

To summarize: the  $B(GT)$  for the transition from  $^{12}\text{B}$  to the  $0_2^+$  state at 2.24 MeV in  $^{12}\text{Be}$  has been extracted using the  $^{12}\text{B}(^7\text{Li},^7\text{Be})$  reaction in inverse kinematics. By combining this results with the known  $B(GT)$  for the transition to the  $0_1^+$  (ground state) in  $^{12}\text{Be}$ , the  $0\hbar\omega$  fractions of the wavefunctions of these  $0^+$  states were determined by comparison with shell-model calculations. It has been demonstrated that GT strengths extracted via charge-exchange reactions at intermediate energies, and in particular the  $(^7\text{Li},^7\text{Be})$  reaction, provide valuable tools for quantifying shell evolution in unstable nuclei, providing complementary information to that obtained with other techniques.

We thank the NSCL staff for their contributions. This work was supported by the US NSF (PHY-0606007, PHY-0822648 (JINA), and PHY-1068217).

---

\* rhiannon.meharchand@gmail.com; Present Address: Los Alamos National Laboratory, Los Alamos, NM 87545, USA

† zegers@nscl.msu.edu

‡ Present Address: Physics Department, Idaho State University, Pocatello, Idaho 83209, USA

§ Present Address: Grand Accélérateur National d'Ions Lourds (GANIL), CEA/DSM-CNRS/IN2P3, Boulevard Henri Becquerel, F-14076 Caen, France

¶ Present Address: Department of Physics, University of

Massachusetts Lowell, Lowell, Massachusetts 01854, USA

\*\* Present Address: CEA, Centre de Saclay, IRFU/Service de Physique Nucléaire, F-91191 Gif-sur-Yvette, France

†† Present Address: Simon Fraser University, Burnaby, British Columbia V5A 1S6, Canada

‡‡ Present Address: Los Alamos National Laboratory, Los Alamos, NM 87545, USA

- [1] D. E. Alburger *et al.*, Phys. Rev. C **17**, 1525 (1978).
- [2] M. Bernas, J. C. Peng, and Nelson Stein, Phys. Lett. **B116**, 7 (1982).
- [3] H. T. Fortune, G.-B. Liu, and D. E. Alburger, Phys. Rev. C **50**, 1355 (1994).
- [4] H. Iwasaki *et al.*, Phys. Lett. **B481**, 7 (2000).
- [5] H. Iwasaki *et al.*, Phys. Lett. **B491**, 8 (2000).
- [6] S. Shimoura *et al.*, Phys. Lett. **B560**, 31 (2003).
- [7] S. Shimoura *et al.*, Phys. Lett. **B654**, 87 (2007).
- [8] A. Navin *et al.*, Phys. Rev. Lett. **85**, 266 (2000).
- [9] S. D. Pain *et al.*, Phys. Rev. Lett. **96**, 032502 (2006).
- [10] R. Kanungo *et al.*, Phys. Lett. **B682**, 391 (2010).
- [11] F. C. Barker, J. Phys. G **2**, 45 (1976).
- [12] H. T. Fortune and R. Sherr, Phys. Rev. C **74**, 024301 (2006).
- [13] F. C. Barker, J. Phys. G **36**, 038001 (2009).
- [14] H. T. Fortune and R. Sherr, J. Phys. G **36**, 038002 (2009).
- [15] H. T. Fortune and R. Sherr, Phys. Rev. C **83**, 044313 (2011).
- [16] C. Romero-Redondo and E. Garrido and D. V. Fedorov and A. S. Jensen, Phys. Rev. C **77**, 054313 (2008).
- [17] G. Blanchon and N. V. Mau and A. Bonaccorso and M. Dupuis and N. Pillet, Phys. Rev. C **82**, 034313 (2010).
- [18] M. Dufour, P. Descouvemont, and F. Nowaki, Nucl. Phys. **A836**, 242 (2010).
- [19] T. Suzuki and T. Otsuka, Phys. Rev. C **56**, 847 (1997).
- [20] T. N. Taddeucci *et al.*, Nucl. Phys. **A469**, 125 (1987).
- [21] F. Ajzenberg-Selove, Nucl. Phys. **A506**, 1 (1990).
- [22] D. J. Morrissey *et al.*, Nucl. Instrum. and Meth. Phys. Res. **B204**, 90 (2003).
- [23] R. G. T. Zegers *et al.*, Phys. Rev. Lett. **104**, 212504 (2010).
- [24] D. Bazin *et al.*, Nucl. Instrum. and Meth. Phys. Res. **B204**, 629 (2003).
- [25] J. Yurkon *et al.*, Nucl. Instrum. and Meth. Phys. Res. **A422**, 291 (1999).
- [26] W. F. Mueller *et al.*, Nucl. Instrum. and Meth. Phys. Res. **A466**, 492 (2001).
- [27] J. Cook and J. Carr, Computer program FOLD (1988). Florida State University (unpublished); based on F. Petrovich and D. Stanley, Nucl. Phys. **A275**, 487 (1977); modified as described in J. Cook *et al.*, Phys. Rev. C **30**, 1538 (1984); R.G.T. Zegers, S. Fracasso, and G. Colò (unpublished).
- [28] B. A. Brown *et al.*, NSCL report MSUCL-1289.
- [29] S. Cohen and D. Kurath, Nucl. Phys. **73**, 1 (1965).
- [30] E. K. Warburton and B. A. Brown, Phys. Rev. C **46**, 923 (1992).
- [31] M. A. Franey and W. G. Love, Phys. Rev. C **31**, 488 (1985).
- [32] A. Nadasen *et al.*, Phys. Rev. C **52**, 1894 (1995).
- [33] C. J. Guess *et al.*, Phys. Rev. C **80**, 024305 (2009).
- [34] A. L. Cole *et al.*, Phys. Rev. C **74**, 034333 (2006).
- [35] Y. Utsuno and S. Chiba, Phys. Rev. C **83**, 021301(R) (2011).